Ruprecht-Karls-Universität Heidelberg
Institut für Informatik
Lehrstuhl für Artificial Intelligence for Programming

Masterarbeit

Signature of warm dark matter in the cosmological density fields extracted using Machine Learning

Name:	Ander Artola
Matrikelnummer:	Matrikelnummer des Autors
Betreuer:	Name des Betreuers
Datum der Abgabe:	dd.mm.yyyy

Ich versichere, dass ich diese Bachelor-Arbeit selbstständig verfasst und nur die angegebenen Quellen und Hilfsmittel verwendet habe.

Heidelberg, dd.mm.yyyy

Zusammenfassung

Dies ist eine Zusammenfassung der Arbeit.

Abstract

This is the abstract.

Contents

1 Introduction **1**

1.1 Cosmological preliminaries 1

1.2 The intergalactic medium 3

1.3 Dark matter 8

1.3.1 Evidence for the inclusion of dark matter in the cosmological model 10

1.3.2 Manifold dark matter candidates 10

1.3.3 Constraining mechanisms for dark matter 10

2 Conclusions **11**

Bibliography **12**

1 Introduction

1.1 Cosmological preliminaries

The currently accepted cosmological model describes space-time as a 4-dimensional Lorentzian manifold equipped with the Robertson-Walker metric [1]

$$\mathrm{d}s^2 = c^2\mathrm{d}t^2 - a(t)^2\left(\frac{\mathrm{d}r^2}{1-kr^2} + r^2\mathrm{d}\Omega^2\right), \tag{1.1}$$

with c the speed of light in vacuum, a the scale factor, k a curvature parameter and $\mathrm{d}\Omega$ the angular volume element in spherical coordinates. The scale factor is taken to be unity at the present time. At time t, a physical (proper) distance l_{phy} is then related to a comoving distance l_{com} by

$$l_{\mathrm{phy}} = a(t)l_{\mathrm{cov}}. \tag{1.2}$$

The physical distance at time t between an observer at $r = 0$ and a point at r is then

$$l_{\mathrm{phy}} = a(t)\int_0^r \frac{\mathrm{d}r}{\sqrt{1-kr^2}} = a(t)\chi(r). \tag{1.3}$$

The Robertson-Walker metric implies that for a radial luminous signal emitted at time t_e and received at time t_0, we have

$$\mathrm{d}s^2 = 0 \implies \frac{\mathrm{d}t_0}{a(t_0)} = \frac{\mathrm{d}t_e}{a(t_e)}. \tag{1.4}$$

As a consequence, the received frequency is redshifted according to

$$1 + z = \frac{\lambda_0}{\lambda_e} = \frac{\nu_e}{\nu_0} = \frac{a(t_0)}{a(t_e)}, \tag{1.5}$$

where z is the redshift.

The time-dependence of physical distances in Equation 1.2 implies that an object whose comoving distance χ to an observer is constant recedes by following the Hubble flow according to

$$v(t) = \dot{a}(t)\chi = \frac{\dot{a}}{a}a\chi = H(t)l_{\rm phy}, \tag{1.6}$$

where $H(t)$ is known as the Hubble factor. Equation 1.6 is known a Hubble's law. At present time, $H(t_0) = H_0$ is referred to as Hubble'2 constant. For historical reasons, it is common to work with the reduced Hubble constant $h = H_0[\mathrm{km/s/Mpc}]/100$. Note that, according to Equation 1.3, and using the Robertson-Walker metric for a radial light signal, we obtain

$$\mathrm{d}\chi = \frac{c\mathrm{d}t}{a} \implies \chi = \int_a^1 \frac{\mathrm{d}a}{a\dot{a}} = \int_0^z \frac{c\mathrm{d}z}{H(z)}. \tag{1.7}$$

As a consequence, the proper line element satisfies

$$\mathrm{d}\chi = \frac{c\mathrm{d}z}{H(z)} = \frac{dl}{a(t)} \implies \frac{\mathrm{d}l}{\mathrm{d}z} = \frac{c}{(1+z)H(z)}, \tag{1.8}$$

which will be useful when integrating quantities along a line of sight. When working with such sightlines in spectroscopy, it is often advantageous to work with velocity units instead of redshifts (or proper distances). Differentiating Equation 1.6 and considering a slow varying Hubble factor around a mean redshift $\overline{z}$, we obtain the following useful expression:

$$\mathrm{d}v = H(\overline{z})\mathrm{d}l = H(\overline{z})\frac{c\mathrm{d}z}{(1+\overline{z})H(\overline{z})} = \frac{c\mathrm{d}z}{1+\overline{z}}. \tag{1.9}$$

The evolution of the scale factor (and hence of the redshift) with time is completely determined by the energy content of the universe through Einstein's field equation, which is known as Friedmann's equation in this context

$$H^2 = H_0^2\left(\Omega_{\rm M}(1+z)^3 + \Omega_{\rm R}(1+z)^3 + \Omega_\Lambda + \Omega_K(1+z)^2\right) = H_0^2E(z)^2, \tag{1.10}$$

where the density parameters Ω are related to the physical densities of the components according to

$$\begin{aligned} \Omega_{\rm M} &= \frac{8\pi G}{3H_0^2}\rho_{M0} \\ \Omega_{\rm R} &= \frac{8\pi G}{3H_0^2}\rho_{R0} \\ \Omega_\Lambda &= \frac{8\pi G}{3H_0^2}\rho_\Lambda \\ \Omega_{\rm K} &= -\frac{k}{H_0^2} \end{aligned} \tag{1.11}$$

In Equation 1.11, ρ_{M} denotes the matter density of the universe, ρ_{R} the radiation density, and ρ_{Λ} the dark energy component. In the following, the values used for the cosmological parameters are $\Omega_m = 0.308, \Omega_\Lambda = 0.692, h = 0.678, \Omega_b = 0.0482, \sigma_8 = 0.829$ and $n = 0.961, \Omega_{\mathrm{K}} \approx 0$, as obtained from CMB measurements by the Planck Collaboration [2]. As we will discuss in Section 1.3, the current cosmological model ΛCDM include a cold dark matter component that dominates over baryonic matter. With the previous cosmological parameters, the matter and cosmological constant are equal when

$$\Omega_{\mathrm{M}}(1+z)^3 = \Omega_\Lambda \implies z \approx 0.3. \tag{1.12}$$

In consequence, at the redshift of interest for this work, $z \sim 4-5$, the universe is well-described as a matter dominated universe.

1.2 The intergalactic medium

As the name suggests, the intergalactic medium (IGM) is the low density part of the Universe content that permeates the space between halos and galaxies [3]. The history of the IGM is closely realted to the formation and evolution of galaxies, with multiple feedback mechanism. For instance, IGM gas can aggregate and provide material to be captured by halos, while the radiation emitted by stars and quasars affect the state of the IGM. At sufficiently early times, all baryons were by definitions part of the IGM, so the IGM represents the primordial material for galaxy formation. Since the IGM has very low densities, its properties are typically probed by the absorbtion of light comming from backgorund sources, such as quasars. To give a rough overview of the properties of the IGM, its typical temperature is $\sim 10^4$ K, with peculiar velocities of $\sim 10-100$ km/s and neutral hydrogen column densities of $\sim 10^{12-17}$ cm^{-2}.

One of the most relevant proccesses in the IGM is ionisation. Consider the hydrogen recombination process:

$$p^+ + e^- \leftrightarrow H + \gamma$$

The ionisation process has two main contribution: collisional ionisation and photo-ionisation.

Collisional ionisation tends to be non-dominant and is due to the collision of a energetic electron with a neutral hydrogen atom. Let Γ_c be the collisional rate, so that the number of collisional ionizsation per unit volume per unit time is $\Gamma_c n_{e^-} n_{HI}$. Photo-ionization is the dominant process and arises from an energetic photon colliding with a neutral hydrogen atom. Let J be the flux of ionizing photons, then the number of photo-ionization per volume per time is $\Gamma_i n_{HI}$ where

$$\Gamma_i = \int_{\nu_t}^{\infty} \frac{4\pi J(\nu)}{ch_{\mathrm{P}}\nu} c\sigma(\nu)\,\mathrm{d}\,\nu \tag{1.13}$$

and ν_t is the threshold frequency for ionizing photons (so, the Rydberg energy). If α is the recombination rate, the number of recombinations per time per volume is $\alpha n_{p^+} n_{e^-}$. The equilibrium equation is the

$$\alpha n_{p^+} n_{e^-} = \Gamma_i n_{HI} + \Gamma_c n_{e^-} n_{HI} \tag{1.14}$$

And so, the neutral hydrogen number density at equilibrium must be:

$$n_{HI} = \frac{\alpha n_{p^+} n_{e^-}}{\Gamma_c n_{e^-} + \Gamma_i} \tag{1.15}$$

Note that here n_{p^+} is the density of free protons. If the gas is highly ionized we can take $n_{e^-} = n_{HI} + n_{p^+} \approx n_{p^+}$ and so, neglecting the collision part:

$$n_{HI} = \frac{\alpha n_{p^+}^2}{\Gamma_i} \tag{1.16}$$

In a dynamic universe, the equilibrium holds provided that the reaction rates are sufficiently large compared to the expansion time-scale H^{-1}. Since photo-ionization dominates, this can be expressed as

$$H^{-1}(z) << \Gamma_i, \tag{1.17}$$

where Γ_i depends on the ionizing photon flux, and so depends on redshift.

Considering that the IGM is made out of fully ionized hydrogen and helium, we have that:

$$n_p = n_H + 2n_{He} \qquad\qquad n_n = 2n_{He} \tag{1.18}$$

The helium weight fraction is then defined as

$$Y = \frac{m_{He}}{m_{He} + m_H} \approx \frac{4n_{He}}{4n_{He} + n_H} = \frac{2n_n}{n_n + n_p} = \frac{2n_n/n_p}{1 + n_n/n_p} \approx 0.25 \tag{1.19}$$

The IGM also contains helium and a small fraction of metals, that contribute to its absorption propoerties.

We are generally interested in matter fluctions of the IGM. Hence, we define the following quantity of interest, called the *baryonic overdensity* field, as

$$\Delta = \frac{\rho}{\bar{\rho}} \tag{1.20}$$

where $\rho(\bar{\rho})$ is the (mean) baryonic density. Let us recover the hydrogen density n_H from the baryonic overdensity Δ, the redshift z and the density parameter Ω_b. First, suppose there is no overdensity so that $\Delta = 1$ and the comoving density is homogeneous. Recall from the mean molecular weight section that

$$\mu_H = \frac{1}{1-Y} = \frac{4}{3} = \frac{\rho_b}{m_p n_H} \tag{1.21}$$

and that

$$\rho_b = \frac{3H^2}{8\pi G}\Omega_b \tag{1.22}$$

so that

$$n_H = \frac{9H^2\Omega_b}{32 m_p \pi G} \tag{1.23}$$

Now, in a matter-dominated universe (for the redshifts we are interested in), Friedmann equation states $H^2 = H_0^2(1+z)^3$. So, we obtain,

$$n_H = \frac{9}{32 m_p \pi G} H_0^2 \Omega_b (1+z)^3 \tag{1.24}$$

and substituting values,

$$n_H = 1.7 \cdot 10^{-7}(1+z)^3 cm^{-3} \tag{1.25}$$

Now if, the hydrogen density is not homogeneous (that is, $\Delta \neq 1$), n_H will be locally modulated by Δ, so that

$$n_H = 1.7 \cdot 10^{-7}(1+z)^3 \Delta \mathrm{cm}^{-3}. \tag{1.26}$$

Since cosmological simulation typically produce as output the baryonic over density Δ, we can use Equation 1.26 to recover the corresponding hydrogren density. The Lyman-α opacity can then be used to estimate the average neutral hydrogen fraction x_{HI}. The evolution of the observed Lyman-α optical depth indicates that the IGM is highly ionized at $z \lessapprox 5.5$, [4], [5]. The two main sources of UV ionising photons are belived to be young galaxies and quasars.

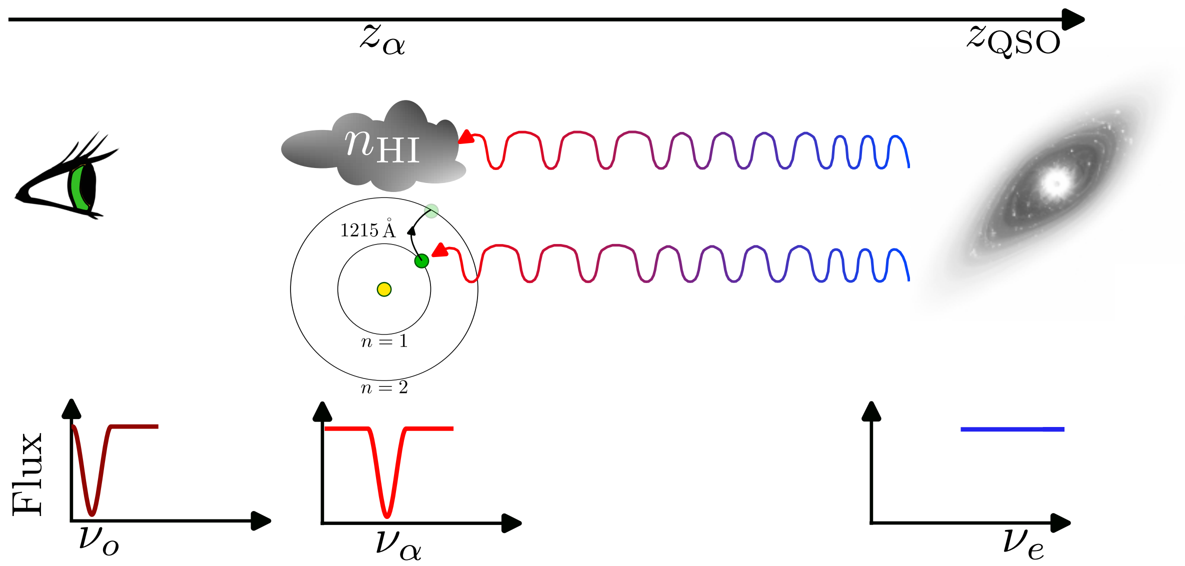

Figure 1.1: Illustration of the Lyman-α absorption by neutral hydrogen at $z = z_\alpha$ in the line of sight of a QSO at $z = z_{\rm QSO}$. In the observer's rest frame, the observed frequency is ν_o. The associated frequency emitted by the QSO is ν_e.

Let us now describe how an intergalactic cloud (with no peculiar velocity) along the line of sight of a quasar affects its spectrum, allowing for a powerful probing mechanism of the IGM. Consider the situation illustrated in Figure 1.1, where a QSO at redshift $z_{\rm QSO}$ emits photons, and consider the propagation of an emitted photon with rest-frame frequency ν_e. Those photons are redshifted and are absorbed in z_α by a neutral hydrogen absorber with local number density $n(z_\alpha)$ producing an absorption feature in the flux at the rest-frame Lyman-α resonance $\lambda_\alpha \approx 1215$Å. The unabsorbed photons are then redshifted and are detected by an observer at $z = 0$ and a frequency ν_o. The relationship between the frequencies mentioned above is then:

$$\nu_o = \frac{\nu_e}{1 + z_e} = \frac{\nu_\alpha}{1 + z_\alpha} \tag{1.27}$$

We are interested in studying the effect of the Lyman-α absorbed at z_α. The observed flux attenuation at the observed frequency ν_0 is then expressed as $\exp(-\tau_\alpha)$, with τ_α the Lyman-α opacity at the observed frequency, which depends on the observer's density and the Lyman-α cross-section $\sigma_\alpha(\nu)$. Observe now that since the Lyman-α cross-section is strongly peaked at the resonance ν_α, but can have a non-zero width, a nearby neutral hydrogen cloud might absorb photons at a redshift different to z_α that would have contributed to the observed flux at frequency ν_o. With this consideration, we integrate over the line of sight to obtain the Lyman-α opacity at the observed frequency

$$\tau_\alpha(\nu_o) = \int_o^{z_{\rm QSO}} n_{\rm HI}(z)\sigma_\alpha[\nu_o(1+z)]{\rm d}z. \tag{1.28}$$

If we now take $\sigma_\alpha(\nu)$ to be a Dirac delta centered at the resonance ν_α, and we integrate Equation 1.28 by using 1.8 we obtain

$$\tau_\alpha(\nu_o) \approx \frac{cn_{\rm HI}(z_\alpha)\sigma_\alpha}{H_0\Omega_{\rm m}^{1/2}(1+z)^{1/3}}, \tag{1.29}$$

where now $\sigma_\alpha = 4.5 \times 10^{-18}{\rm cm}^2$ is to total Lyman-α cross-section. Equation 1.29 is known as the Gunn-Peterson approximation for the Lyman-α opacity of the IGM [6]. Equation 1.29 demonstrates that quasar spectra are a useful probe of the intergalactic neutral hydrogen density.

A more precise analysis of Equation 1.28 can be done if we do not approximate σ_α as a Dirac delta. Instead, we can include the two main broadening effects on the absoprtion corss-section: the natural broadening and the thermal broadening. The natural broadening is a result of quantum processes and generates a Lorentzian profile, while the thermal one is due to the microscopic Doppler effect of thermal motion and generates a Gaussian profile. The resulting combinatin of both the Lorentzian and Gaussian profiles is known as a Voigt profile. It is a non-analytical function with a Gaussian-like shape but heavier tails:

$$V(x,y) = \frac{Y}{\pi}\int_{-\infty}^{\infty}\frac{e^{-t^2}}{(x-t)^2+y^2}dt. \tag{1.30}$$

The Lyman-α absoprtion cross-section described by the Voigt profile is then

$$\sigma_\alpha(\nu) = \frac{cI_\alpha}{b\sqrt{\pi}}V\left(\frac{x(\nu-\nu_\alpha)}{b\nu_\alpha}, \alpha\right), \tag{1.31}$$

where $b = \frac{\sqrt{2k_BT}}{m_p}$ is the Doppler parameter at temperature T, $\nu_\alpha \approx 2.47 \times 10^{15}$ Hz is the $Lyman - \alpha$ frequency, $I_\alpha \approx 4.45 \times 10^{-18}$ cm^{-2} is the total absoprtion cross-section [3] and α is the recombination coefficient, which also depends on the temperature. The Lyman-α cross-section is then peaked at the resonant frequency, and broadened by the temperature and the recombination rate. Now, consider a sightline of gas absorbing Lyman-α photons. Peculiar bulk velocities v of the gas will add an additional Doppler effect in the cross-section as

$$\sigma_\alpha(\nu) = \frac{cI_\alpha}{b\sqrt{\pi}} V\left(\frac{x(\nu-\nu_\alpha)}{b\nu_\alpha} + \frac{v}{b}, \alpha\right). \tag{1.32}$$

We can now integrate Equation 1.32 along the sightline to obtain the Lyman-α opcaity τ as

$$\tau = \int n(t)\sigma_\alpha(\nu_\alpha a(t_0)/a(t))dt, \tag{1.33}$$

where n is the neutral hydrogen density and t_0 the emisison time. Recalling that the comoving distance x is related to redshift and time as

$$dx = \frac{c}{H(z)}dz = c(1+z)dt, \tag{1.34}$$

we get that the Lyman-α optical depth τ can be obtained from the neutral hydrogen gas properties along the sightline as follows:

$$\tau(z_0) = \frac{cI_\alpha}{\sqrt{\pi}} \int dx \frac{n_{\mathrm{H}}[x, z(x)]}{b[x, z(x)][1+z(x)]} \times V\left\{\frac{c[z(x)-z_0]}{b[x, z(x)](1+z_0)} + \frac{v[x, z(x)]}{b[x, z(x)]}, \alpha\right\} \tag{1.35}$$

where n_{H} is the neutral hydrogen density, $b = \sqrt{\frac{2k_BT}{m_p}}$, v is the peculiar velocity along the sightline, m_p is the proton mass, k_B is Boltzmann's constant, α is the recombination coefficient, c is the speed of light, I_α is the total cross-section for Lyman-α absorption and V is the Voigt function [7]. Since the Lyman-α flux $F = e^{-\tau}$ field depends on the properties of the absorbing gas, it contains information about the state of the IGM

1.3 Dark matter

Many aspects of the large-scale structure of the Universe can be understood by including a *cold dark matter* (CDM) component that represents $\sim 26\%$ of the critical density [2]. In the standard cosmological model, ΛCDM, dark matter is an important ingredient for structure formation in the Early Universe. However, its precise nature remains an outstanding problem both in cosmology and particle physics. With more exotic DM candidates, such as primordial black holes, heavily constrained, it is likely that DM consists of some undiscovered elementary particle(s) produced early in the history of the universe [8]. There are multiple pieces of evidence supporting the CDM model, including the rotation curves of spiral galaxies and the kinematics of colliding clusters such as the Bullet cluster [9], [10].

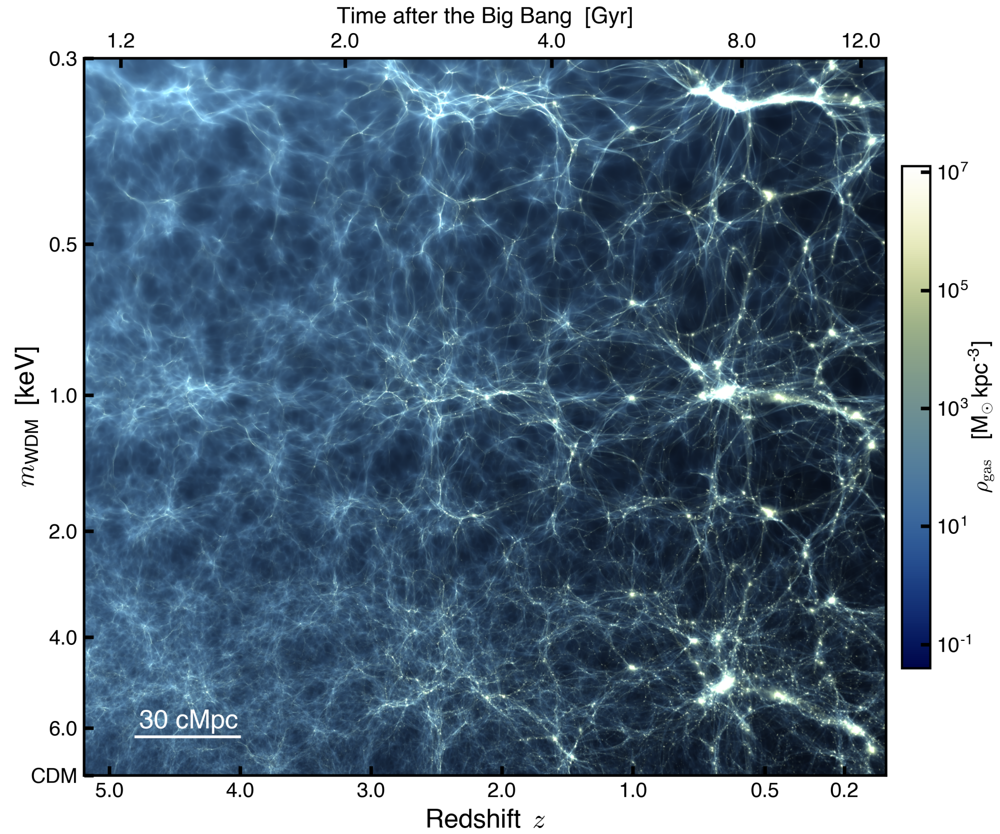

Figure 1.2: Baryonic density plot of the IGM as a function of redshift, and the WDM model mass. On the horizontal axis, the time evolution shows how gravity collapses dense regions into structures. On the vertical axis, the WDM free-streaming length suppress small-scale clustering. Extracted from [18].

On large scales, the predictions of ΛCDM have been amply tested and are in good agreement with observations [11],[12], [13]. In contrast, on scales smaller than ~ 10 kpc, potential tensions between CDM predictions and observations might exist, including the "core-cusp" problem related to the DM density profile in halos, or the "too big to fail" problem linked to the number density of high-luminosity satellites in sub-halos [14], [15], [16]. Even if the inclusion of complex baryonic feedback processes can alleviate the aforementioned potential discrepancies, alternative models to CDM are worth exploring [17].

discuss villa plot role on the IGM TEST free straming length

1.3.1 Evidence for the inclusion of dark matter in the cosmological model

1.3.2 Manifold dark matter candidates

WDM and the papers about neutrinos etc.

1.3.3 Constraining mechanisms for dark matter

previous efforts, lyman-alpha forest, other techniques for DM being black holes with lensing

2 Conclusions

Bibliography

[1] Sean M. Carroll. *Spacetime and Geometry: An Introduction to General Relativity*. Cambridge University Press, 2019.

[2] Planck Collaboration, P. A. R. Ade, N. Aghanim, C. Armitage-Caplan, M. Arnaud, et al. "Planck 2013 results. XVI. Cosmological parameters". In: *APP* 571, A16 (Nov. 2014), A16. DOI: 10.1051/0004-6361/201321591. arXiv: 1303.5076 [astro-ph.CO].

[3] Houjun Mo, Frank van den Bosch, and Simon White. *Galaxy Formation and Evolution*. Cambridge University Press, May 2010. ISBN: 9780511807244. DOI: 10.1017/cbo9780511807244. URL: http://dx.doi.org/10.1017/CBO9780511807244.

[4] Robert H. Becker, Xiaohui Fan, Richard L. White, Michael A. Strauss, Vijay K. Narayanan, et al. "Evidence for Reionization at z$\sim$ 6: Detection of a Gunn-Peterson Trough in a $z = 6.28$ Quasar". In: *The Astronomical Journal* 122.6 (Dec. 2001), pp. 2850–2857. ISSN: 0004-6256. DOI: 10.1086/324231. URL: http://dx.doi.org/10.1086/324231.

[5] Ian D. McGreer, Andrei Mesinger, and Valentina D'Odorico. "Model-independent evidence in favour of an end to reionization by z $\approx$ 6". In: *MNRAS* 447.1 (Feb. 2015), pp. 499–505. DOI: 10.1093/mnras/stu2449. arXiv: 1411.5375 [astro-ph.CO].

[6] James E. Gunn and Bruce A. Peterson. "On the Density of Neutral Hydrogen in Intergalactic Space." In: *APJ* 142 (Nov. 1965), pp. 1633–1636. DOI: 10.1086/148444.

[7] T. Roy Choudhury, R. Srianand, and T. Padmanabhan. "Semianalytic Approach to Understanding the Distribution of Neutral Hydrogen in the Universe: Comparison of Simulations with Observations". In: *The Astrophysical Journal* 559.1 (Sept. 2001), pp. 29–40. ISSN: 1538-4357. DOI: 10.1086/322327. URL: http://dx.doi.org/10.1086/322327.

[8] Pablo Villanueva-Domingo, Olga Mena, and Sergio Palomares-Ruiz. “A Brief Review on Primordial Black Holes as Dark Matter”. In: *Frontiers in Astronomy and Space Sciences* 8 (May 2021). ISSN: 2296-987X. DOI: `10.3389/fspas.2021.681084`. URL: `http://dx.doi.org/10.3389/fspas.2021.681084`.

[9] Julio F. Navarro, Carlos S. Frenk, and Simon D. M. White. “The Structure of Cold Dark Matter Halos”. In: *The Astrophysical Journal* 462 (May 1996), p. 563. ISSN: 1538-4357. DOI: `10.1086/177173`. URL: `http://dx.doi.org/10.1086/177173`.

[10] W. J. G. de Blok, F. Walter, E. Brinks, C. Trachternach, S-H. Oh, and R. C. Kennicutt. “HIGH-RESOLUTION ROTATION CURVES AND GALAXY MASS MODELS FROM THINGS”. In: *The Astronomical Journal* 136.6 (Nov. 2008), pp. 2648–2719. ISSN: 1538-3881. DOI: `10.1088/0004-6256/136/6/2648`. URL: `http://dx.doi.org/10.1088/0004-6256/136/6/2648`.

[11] N. Dalal and C. S. Kochanek. “Direct Detection of Cold Dark Matter Substructure”. In: *The Astrophysical Journal* 572.1 (June 2002), pp. 25–33. ISSN: 1538-4357. DOI: `10.1086/340303`. URL: `http://dx.doi.org/10.1086/340303`.

[12] L. Van Waerbeke, Y. Mellier, and H. Hoekstra. “Dealing with systematics in cosmic shear studies: New results from the VIRMOS-Descart survey”. In: *Astronomy and Astrophysics* 429.1 (Dec. 2004), pp. 75–84. ISSN: 1432-0746. DOI: `10.1051/0004-6361:20041513`. URL: `http://dx.doi.org/10.1051/0004-6361:20041513`.

[13] Daniel J. Eisenstein, Idit Zehavi, David W. Hogg, Roman Scoccimarro, Michael R. Blanton, et al. “Detection of the Baryon Acoustic Peak in the Large-Scale Correlation Function of SDSS Luminous Red Galaxies”. In: *The Astrophysical Journal* 633.2 (Nov. 2005), pp. 560–574. ISSN: 1538-4357. DOI: `10.1086/466512`. URL: `http://dx.doi.org/10.1086/466512`.

[14] Ben Moore. “Evidence against dissipation-less dark matter from observations of galaxy haloes”. In: *Nature* 370.6491 (Aug. 1994), pp. 629–631. ISSN: 1476-4687. DOI: `10.1038/370629a0`. URL: `http://dx.doi.org/10.1038/370629a0`.

[15] Michael Boylan-Kolchin, James S. Bullock, and Manoj Kaplinghat. “Too big to fail? The puzzling darkness of massive Milky Way subhaloes”. In: *Monthly Notices of the Royal Astronomical Society: Letters* 415.1 (July 2011), pp. L40–L44. ISSN: 1745-3925. DOI: `10.1111/j.1745-3933.2011.01074.x`. URL: `http://dx.doi.org/10.1111/j.1745-3933.2011.01074.x`.

[16] David H. Weinberg, James S. Bullock, Fabio Governato, Rachel Kuzio de Naray, and Annika H. G. Peter. “Cold dark matter: Controversies on small scales”. In: *Proceedings of the National Academy of Sciences* 112.40 (Feb. 2015), pp. 12249–12255. ISSN: 1091-6490. DOI: 10.1073/pnas.1308716112. URL: http://dx.doi.org/10.1073/pnas.1308716112.

[17] M. Vogelsberger, S. Genel, V. Springel, P. Torrey, D. Sijacki, D. Xu, G. Snyder, S. Bird, D. Nelson, and L. Hernquist. “Properties of galaxies reproduced by a hydrodynamic simulation”. In: *Nature* 509.7499 (May 2014), pp. 177–182. ISSN: 1476-4687. DOI: 10.1038/nature13316. URL: http://dx.doi.org/10.1038/nature13316.

[18] Bruno Villasenor, Brant Robertson, Piero Madau, and Evan Schneider. “New constraints on warm dark matter from the Lyman-alpha forest power spectrum”. In: *Physical Review D* 108.2 (July 2023). ISSN: 2470-0029. DOI: 10.1103/physrevd.108.023502. URL: http://dx.doi.org/10.1103/PhysRevD.108.023502.